ISSN 1063-7850, Technical Physics Letters, 2010, Vol. 36, No. 12, pp. 1072–1075. © Pleiades Publishing, Ltd., 2010.
Original Russian Text © A.V. Garbaruk, D.A. Demidov, S.G. Kalmykov, M.E. Sasin, 2010, published in Pis'ma v Zhurnal Tekhnicheskoĭ Fiziki, 2010, Vol. 36, No. 23, pp. 9–16.

Numerical Simulation of Gas-Jet Target in the Laser-Produced-Plasma Short-Wave-Radiation Source¶

A. V. Garbaruk[a], D. A. Demidov[a], S. G. Kalmykov[b], and M. E. Sasin[b]

[a] *St. Petersburg State Polytechnical University, St. Petersburg, 195251 Russia*

[b] *Ioffe Physical Technical Institute, Russian Academy of Sciences, St. Petersburg, 194021 Russia*

e-mail: Serguei.Kalmykov@mail.ioffe.ru

Received June 18, 2010

Abstract—Numerical simulation of Xe gas jet, outflowing from a nozzle into the vacuum and considered as a target in the LPP radiation source, has been carried out. Different nozzle configurations and different gas conditions before the nozzle have been considered. A criterion based on the simulation results and describing observable plasma radiation intensity has been proposed. The criterion makes it possible to select an optimum configuration for a further experimentation. Results of the calculation are compared with earlier published experimental data.

DOI: 10.1134/S1063785010120023

A trend to enhance short-wave radiation output from the plasma in the source under consideration implies increasing the gas-jet-target density [1] that, in turn, results in rise of the peripheric gas density and thereby in rise of undesirable self-absorption of the radiation as it was demonstrated in experiments [2–4]. Also, in the same experiments the plasma has been shown to be very extended along the laser beam; the fact that devaluates in some extent the laser plasma as a point radiation source due to enhanced light loss in the optical system. Obtaining a target jet with increased central density and the reduced peripheric one can be considered as an effective method to supress both the phenomena.

Adiabatic expansion of the gas, outflowing from supersonic nozzles, forms a jet where two specific parts can be distinguished—a dense and cold core which dissipates relatively slowly when moving away from the nozzle, and a warm peripherical gas which fast expands and loses its density. An optimum target jet structure is expected to exist at some outflow modes. Search of such modes is the goal of the simulation.

In the present work, numerical solution of steady Navier–Stocks equations, which simulated an axisymmetic compressible gas (Xe) outflow from a nozzle to the vacuum, was performed. As the nozzle flow transition time was estimated to be $\sim 1 \times 10^{-2}$ ms under the circumstances, the stationarity looked like a reasonable assumption for the vacuum vessel of 25 cm in dimensions and the gas pulse time of millisecond range (see characteristic experimental setup parameters in [5]). Finite volume method with second order approximations for convective and viscous terms was used. Block-structured grid size was 20 to 100 kilonodes. Stagnation pressure and temperature was specified on the inlet boundary (nozzle inlet); on the outlet one, *a fortiori* low static pressure (1×10^{-4} Pa) was set. Non-slip adiabatic boundary conditions were used on the material walls. The computational results were presented as a two-coordinate $[r, x]$ field where all flow parameters (the atomic concentration included) were defined in each point.

Obvious model defect was neglect of the condensation which could occur in the central low-temperature core. However, estimates made [6] predicted only $\sim 10^{-4}$ portion of the jet matter to be condensed under the circumstances, and so the condensation could be considered as negligible.

At the low outlet boundary pressure above, a discontinuity of a medium had to be expected. Therefore, to define boundaries of a zone where the continuity conditions were valid, and also to examine effect of the boundary conditions chosen, and to determine acceptable grid parameters, a series of preliminary calculations has been realized. The main bulk of computations has been carried out for 7 different nozzle configurations (one of them being cylindrical and other six being Laval nozzles, see the table) at inlet pressures within $P_0 = 1$–10 atm and temperatures of 200 and 293 K.

Figure 1 displays gas density radial profile variations subject to the nozzle configuration. A nozzle group composed of nos. 1, 5 and 7 (see the table) seems to be the most satisfying the optimization requirements due to their narrowest profiles among others.

¶The article was translated by the authors.

The density profiles calculated at different distances from the nozzle edge show the gas density and its radial distribution to vary relatively slightly only within lengths of one outlet diameter, at longer distances the profiles spread and the gas density drops. The point located at that distance, e.g., $\Delta x = 1$ mm for the nozzle no. 1, is evidently optimum for the laser beam to be focused on it.

Significant radial profile variability makes difficult comparison of the nozzles and their operational modes. To make the selection procedure more objective and unambiguous, an optimization parameter is required that would allow to estimate the profile quality as a whole from the point of view of an external observer.

In the present work, the plasma induced with the laser beam is assumed to be asisymmetric, r_{pl} being its radius. The plasma axis (i.e. the laser beam one) is perpendicular to that of the gas jet but, in the general case, not necessarily intersects it. The line of observation is the third perpendicular and intersects two other axes. Let Δr denominate the distance between the axes, then $\Delta r > 0$ means the plasma axis is displaced away from the gas jet to the observer's side.

Since radiation events take place at binary collisions, the radiation intensity of a transparent plasma (what is valid at least for the continual radiation—see the corresponding estimation in [1]) is proportional to the squared atomic concentration integrated along the plasma diameter, $d_{pl} = 2r_{pl}$: $\langle n^2 l\rangle_{pl} \equiv \int n^2\, dl$. When propagating to the observer, the radiation passes through the unionized peripherical gas and is partially absorbed in it. The transmitted portion is $I/I_0 = \exp\{-\sigma_{abs}\langle nl\rangle_{peri}\}$, where $\langle nl\rangle_{peri} \equiv \int n\, dl$ is integral along the line of sight from the plasma boundary faced to the observer up to the external boundary of whole the gas dynamics problem, and σ_{abs} is the absorption cross-section (in the present work $\sigma_{abs} = 2.365 \times 10^{-17}$ cm^2—maximum value within the Xe absorption band). Then, $F = \langle n^2 l\rangle_{pl}\exp\{-\sigma_{abs}\langle nl\rangle_{peri}\}$ is a composite integral parameter to which the observed plasma radiation intensity is proportional.

Comparison between F-values for different nozzles at different assumed plasma radii (r_{pl} = 50–300 μm) has shown the mentioned above nozzles nos. 1, 5 and 7 to be optimum for the case when plasma and jet axes intersect (i.e. $\Delta r = 0$), and for each given nozzle, the function F vs. pressure exhibits a maximum which, for the case of the nozzle no. 1 for example, is located at P_0 = 6–8 atm. For comparison, the jet produced with the nozzle no. 2 has wider radial profile and higher central concentration with maximum F located at $P_0 = 2$ atm but the maximum value is less than that for the nozzle no. 1 approximately by two times. It is noteworthy that for the central plasma column position, $\Delta r = 0$, transmission of the radiation through the peripherical gas is relatively small, 15 to 35%, at all optimal pressures.

Geometrical parameters of nozzles (r_{cr} and r_{ex} are nozzle radii at critical and outlet sections, respectively, l is nozzle length)

Nozzle number	r_{cr}, mm	r_{ex}, mm	l, mm
1	0.1	0.55	13
2	0.2	0.55	13
3	0.1	0.1	13
4	0.1	1.1	13
5	0.1	0.55	17
6	0.1	0.55	6
7	0.1	0.55	25

If the plasma column axis is shifted to the observer's side, $\Delta r > 0$, one can expect the effect of the corresponding relatively small decrease in the plasma density to be exceeded with that of more significant increase in transparency of the gas between the plasma and the observer. Indeed, Fig. 2 shows plasma axis shifting to result in increased radiation output for all the nozzles, but in this case, the nozzle no. 2 at higher pressures appears to be the most optimum. As would be expected, for the geometries with shifted plasma axis, the transmission at the optimal pressures is higher, 40–70%, than that for $\Delta r = 0$.

Two experiments described in [2] and in [3, 4] can be analyzed with the aid of the computational method proposed here. An additional simulation has been realized for the cylindrical nozzle ($\Delta r = 0.2$ mm, $l =$

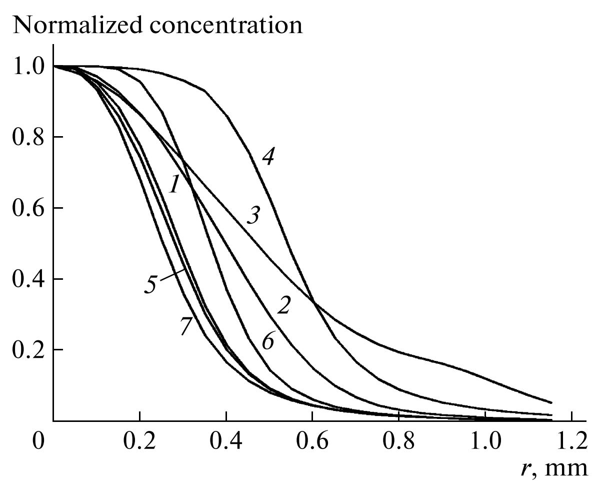

Fig. 1. Atomic concentration radial profiles for different nozzles. Numbers at curves are those of nozzle configurations in accordance with the table. Inlet temperature and pressure are $T_0 = 293$ K and $P_0 = 5$ atm, respectively. Distance from the nozzle edge is $\Delta x = 1$ mm. Central concentration values (in 10^{18} cm^{-3} units): (*1*) 3.4; (*2*) 8.2; (*3*) 0.9; (*4*) 1.2; (*5*) 3.5; (*6*) 2.5; (*7*) 3.7.

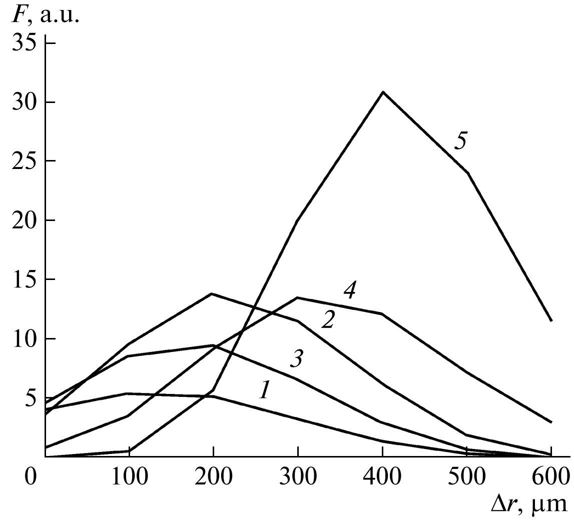

Fig. 2. Parameter F representing the observable plasma emittance vs. displacement of the plasma axis with respect to the jet one, Δr. Distance from the nozzle edge is x = 1 mm, plasma body radius is r_{pl} = 200 μm.
Curves *1*, *2*, *3* are calculated for the nozzle no. 1 at inlet gas parameters P_0 = 5 atm and T_0 = 293 K (*1*), P_0 = 10 atm and T_0 = 293 K (*2*), P_0 = 5 atm and T_0 = 200 K (*3*); curves *4* and *5* describe nozzle no. 2 jets at P_0 = 5 atm and T_0 = 293 K (*4*), P_0 = 10 atm and T_0 = 293 K (*5*).

10 mm) from [2] and the F-parameter has then been calculated under conditions of the experiment (P_0 = 10 atm, x = 0.5 mm, $r_{pl} \approx$ 100 μm). The conic nozzle from [3, 4] is very similar to the nozzle no. 2 from the table (with the only little difference: in [3, 4] the nozzle length is l = 10 mm but the nozzle no. 2 length is l = 13 mm), so the latter is used furthermore in the simulation of the experiment [3, 4]. Conditions were almost identical in both the experiments but in [3, 4] the distance from the nozzle edge was x = 1 mm.

Radial Xe density profiles are shown on Fig. 3a for both the experiments. They differ only within a narrow paraxial zone with 300 μm radius. Behaviour of the F-parameter, represented on Fig. 3b, corresponds qualitatively to variations of the experimentally observed short-wave plasma emittance. In fact, at the central plasma position, Δr = 0, F-value calculated for the nozzle no. 2 is by 2.5 times as high than that for the nozzle in [2]. Experimentally, the short-wave plasma radiation was not in the least observed in the work [2] unlike the experiment [3, 4] with the central plasma location where it was quite observable. When the plasma column axis is displaced from its central position towards the observer, the F-parameter increases and reaches its maximum value at r = 350–550 μm (Fig. 3b, curve *2*)—approximately in the same place where experimentally observed peak of the plasma radiation was located in [3, 4]. However, in the experiment, the plasma radiation signal increased by 3–4 times, whereas the rise of the calculated F-parameter

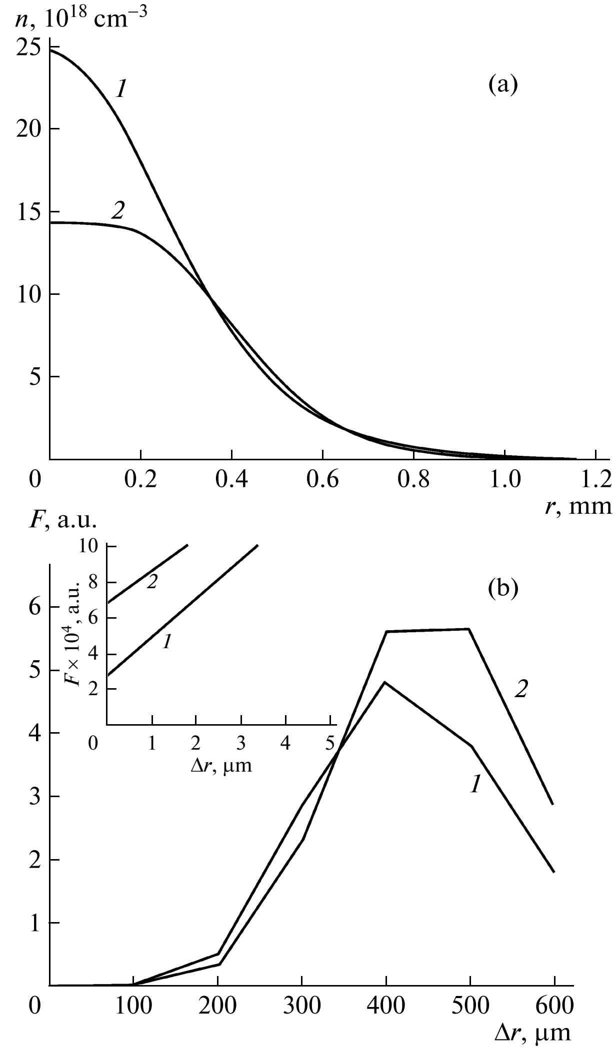

Fig. 3. Simulation results for the experiments described in [2] (curves *1*) and in [3, 4] (curves *2*). Inlet gas parameters are P_0 = 10 atm, T_0 = 293 K, plasma radius is r_{pl} = 100 μm. Distances from the nozzle edge correspond to those in the real experiments: Δx = 0.5 mm for curves *1* and x = 1 mm for curves *2*. (a) Xe atomic concentrations vs. radius. (b) F-parameter vs. Δr, the distance between plasma and jet axes. Shown on the insertion is part of the plot at Δr close to zero, i.e. at the central position of the plasma column.

amounts to almost four orders of magnitude. Moreover, data from [3, 4] evidenced the plasma radiation continued to be observable even when the plasma was located on the back side of the jet and was shaded from observation.

An apparent explanation is what the plasma column had a long extension along the laser beam, about 1–1.5 mm as it has been demonstrated in [2–4], and its ends, distant from the focus, were surrounded with rarefied, weakly absorbing gas at any plasma location relative to the jet and hence remained visible with an uncollimated short-wave-radiation sensor. On the contrary, in the present work the *F*-parameter is calculated for a single observation beam passing through the plasma column center. However, the described computational method could be modified so that *F*-values for many different observation beams were summed up, thus simulating whole solid angle of a sensor.

ACKNOWLEDGMENTS

Authors are grateful to V. G. Kapralov for attracting their attention to the publication [2].

This study was supported by the International Science and Technology Center (ISTC project no. 3857).

REFERENCES

1. S. G. Kalmykov, Pis'ma Zh. Tekh. Fiz. **35** (21), 97 (2009) [Tech. Phys. Lett. **35**, 1020 (2009)].
2. V. G. Kapralov, R. Korde, V. E. Levashov, A. S. Pirozhkov, and E. N. Ragozin, Kvantovaya Electron. **32** (2), 149 (2002) [Quant. Electron. **32**, 149 (2002)].
3. K. N. Mednikov, V. E. Levashov, A. S. Pirozhkov, and E. N. Ragozin, *Nanophysics and Nanoelectronics: The 9th Int. Symp. (March 25–29, 2005, Nizhni Novgorod, Russia)*, Part 2, p. 499 [in Russian].
4. V. E. Levashov, K. N. Mednikov, A. S. Pirozhkov, and E. N. Ragozin, Kvantovaya Electron. **36** (6), 549 (2006) [Quant. Electron. **36**, 549 (2006)].
5. S. V. Bobashev, A. P. Zhevlakov, S. G. Kalmykov, I. M. Roiz, R. P. Seisyan, and G. K. Tumakayev, Abstracts of Papers. RUSNANOTECH-08: Int. Forum on Nanotechnology (December 3–5, 2008, Moscow, Russia), Part 2, p. 225 [in Russian].
6. A. S. Boldarev, V. A. Gasilov, V. E. Levashov, K. N. Mednikov, A. S. Pirozhkov, M. S. Pirozhkova, and E. N. Ragozin, Kvantovaya Electron. **34** (7), 679 (2004) [Quant. Electron. **34**, 679 (2004)].